Effect of swift heavy ions irradiation on the migration behavior of strontium implanted into polycrystalline SiC

H.A.A. Abdelbagi[1,2], V.A. Skuratov [3,4], S.V. Motloung[5], E.G. Njoroge[1], M. Mlambo[1], T.T. Hlatshwayo[1], J.B. Malherbe[1]

[1]*Physics Department, University of Pretoria, Pretoria 0002, South Africa*

[2]*Physics Department, Shendi University, Shendi, Sudan*

[3]*Joint Institute for Nuclear Research, Dubna, Russia*

[4]*National Research Nuclear University MEPhI, Moscow*

[5]*Department of Physics, Nelson Mandela Metropolitan University (NMMU), P. O. Box 77000, Port Elizabeth 6031, South Africa*

ABSTRACT

The influence of swift heavy ions (SHIs) irradiation on the microstructure and the migration behavior of strontium (Sr) implanted into polycrystalline SiC were investigated using Rutherford backscattering spectrometry (RBS), Raman spectroscopy and scanning electron microscopy (SEM). The as-implanted and SHIs irradiated samples were vacuum annealed from 1100 to 1500 ºC in steps of 100 ºC for 5 hours. Implantation of strontium (Sr) amorphized the SiC, while SHIs irradiation of the as-implanted SiC resulted in limited recrystallization of the initially amorphized SiC. Annealing at 1100 ºC already caused recrystallization in both the irradiated and un-irradiated but implanted with Sr samples. At 1500 ºC, a carbon layer appeared on the surface of the irradiated and un-irradiated but implanted with Sr samples. This was due to the decomposition of the SiC and subsequent sublimation of silicon leaving a free carbon layer on the surface. SHIs irradiation alone induced no change in the implanted Sr. Annealing the samples at 1400 ºC caused a release of all implanted strontium in the SHIs irradiated samples, while 55% of implanted strontium was released in the un-irradiated but implanted with Sr samples. The enhanced Sr releasing in SHIs irradiated samples was explained in terms of the high number of pores in the irradiated samples compared to fewer pores in the un-irradiated but implanted with Sr samples. The results show that more Sr was released in the irradiated SiC samples.

Keywords: SHI, RBS, SiC.

*Corresponding author: heshamabdelbagi100@gmail.com

1. Introduction

The Pebble Bed Modular Reactor (PBMR) is one of the high temperature gas-cooled reactors (HTGRs) [1-4]. This PBMR uses the tri-isotropic (TRISO) particle which consists of the fuel kernel (UO_2) encapsulated with four chemical vapour deposited (CVD) layers [5]. First layer is a porous carbon buffer layer and it is designed to reduce recoiling fission products (FPs) and accommodates internal gas buildup. The second and third layers are the inner pyrolytic carbon (IPyC) layer and silicon carbide (SiC) layer, the IPyC layer acts as a diffusion barrier to most non-metallic FPs while the SiC layer is the main diffusion barrier to FPs. The fourth layer is an outer pyrolytic carbon (OPyC) layer that protects SiC. More than 200 SiC polytypes can exist depending on the stacking sequence and on the growth condition in the CVD reaction chamber (i.e. temperature of reaction and pressure) [6]. 3C, 4H, 6H and 15R-SiC are commonly found when fabricated by the CVD process [7]. The 3C-SiC is the preferred polytype for high temperature nuclear reactor applications due to it is higher (defect) radiation resistance against neutron bombardment [6, 8-9]. TRISO particles offer unparalleled containment of fission products in extreme environments of 900-1300 ºC under normal operating conditions and is extremely robust during accident conditions, i.e. above than 1600 °C [3]. During operation, TRISO particles retain most of the radiological important FPs. However, Silver (Ag), strontium (Sr) and europium (Eu) have been observed to be release through intact SiC layer [10]. Extensive studies have been performed to explain the transport mechanism of Ag through SiC [11-14], while little is known about the other FPs such as europium and strontium [3-4,10,15-17]. Radioactive isotopes of strontium can pose important radiological health concerns if released from reactors [18]. This is due to its chemical similarity to calcium, which causes it to be deposited in bones. This makes strontium one of the key FPs whose transport properties in the TRISO particle need to be investigated.

During fission reactions, different nuclei with different energies are released. The energies of these nuclei are in the order of 100 MeV i.e. the energy range of swift heavy ions (SHIs). The fission reaction occurs in the kernel of TRISO particle (UO_2) when a uranium nucleus absorbs a slow neutron. Then it became unstable and splits into smaller nuclei releasing two or three neutrons. The SHIs lose their energy firstly by colliding

with outer electrons of the target material (electronic stopping), later by transferring the energy into the target atom as a whole (nuclear stopping).

The energy loss of SHIs as they are traversing through SiC layer can cause changes in the structure of SiC. No ion tracks have been observed in the SiC for SHI, even up to the practical upper limit of electronic stopping power for SiC, S_e = 34 keV/nm [19,20]. Hlatshwayo et *al.* [21,22] firstly created damage in polycrystalline SiC by irradiating with low energy ions and subsequently irradiated the sample with SHIs. Transmission electron microscopy (TEM) and Raman spectroscopy revealed that the low energy irradiation amorphized SiC while SHIs of the initially amorphized layer caused recrystallization in the form of randomly orientated nanocrystallites. The results were explained in terms of thermal spike model [23]. These structural changes by SHIs irradiation might influence the migration behavior of FPs in SiC. As extensively reviewed in [3] the microstructure of SiC can affect the migration behavior of FPs. Recently, few studies have investigated the migration behavior of different FPs in SiC after SHIs irradiation. No diffusion of implanted I, Kr and Xe in SiC has been detected after SHI irradiation at room temperature and at 500 ^{o}C [21-22,24]. Apart from the study on the effect of carbon ions irradiated in Ag implanted SiC, no other post SHI irradiation annealing results have been reported [25].

The purpose of this paper is to investigation the structural changes in Sr (360 keV) irradiated polycrystalline SiC and in Sr (360 keV) followed by Xe (167 MeV) irradiated polycrystalline SiC. Raman spectroscopy and scanning electron microscopy have been used to study the structure of both samples before and after annealing. Finally, the migration behaviour of Sr were investigated in both samples.

2. Experimental Method

In this study, the polycrystalline CVD-SiC wafers from Valley Design Corporation were used. The SiC wafers were characterized using scanning electron microscopy (SEM), electron backscatter diffraction (EBSD) and were found to be composed of mainly 3C-SiC, i.e. a cubic lattice structure, but some hexagonal crystallites were also present [12]. The as-received samples were implanted with 360 keV Sr^+ ions to a fluence of 2×10^{16} cm^{-2} in vacuum at room temperature at the Friedrich-Schiller-

University Jena, Germany. The implantation was performed at room temperature in order to amorphize the implanted layer.

Some of the implanted samples were irradiated with 167 MeV Xe^{+26} ions to a fluence of 3.4×10^{14} cm^{-2} and 8.3×10^{14} cm^{-2} in vacuum at room temperature using the IC-100 FLNR cyclotron in JINR, Dubna, Russia. This was done to compare both the microstructure of the substrates and the migration behavior of Sr in the initially amorphous SiC layer (in the as-implanted) and SHIs irradiated SiC.

Both samples were subjected to isochronal annealing at temperatures from 1100 to 1500 ^{o}C in steps of 100 ^{o}C for 5 hours using a high vacuum computer-controlled *Webb 77* graphite furnace. The as-implanted, implanted then irradiated and annealed samples were characterized by Raman spectroscopy, SEM and Rutherford backscattering spectrometry (RBS). Raman analysis was recorded using a T64000 series II triple spectrometer system from HORIBA Scientific, Jobin Yvon Technology. The 514.3 nm laser line of a coherent Innova® 70C series Ar^{+} laser (spot size ~ 2 µm) with a resolution of 2 cm^{-1} in the range of 200 cm^{-1} – 1800 cm^{-1} was used. The measurements were obtained in a backscattering configuration with an Olympus microscope attached to the instrument (using an LD 50x objective). The laser power was set at 1.7 mW. An integrated triple spectrometer was used in the double subtractive mode to reject Rayleigh scattering and dispersed the light onto a liquid nitrogen cooled Symphony CCD detector. The Raman spectra were recorded under these conditions and normalized to have the same scale. Some of the Raman peaks were fitted to either a Gaussian or Lorentz function to determine the width (i.e. FWHM) of the peak. SEM analysis was performed using a high-resolution Zeiss Ultra Plus 55 field emission scanning electron microscope (FESEM) operated at 2 kV under vacuum. The changes in the Sr profiles on irradiated and un-irradiated samples before and after annealing were monitored by RBS using He^{+} ions of 1.6 MeV. The backscattered He^{+} ions were detected using a silicon surface barrier detector set at a 165° and charge of 8 µC was collected per measurement. The RBS Sr profiles in energy channels were converted into depth using energy loss data and the density of SiC (3.21 gcm^{-3}).

3. Results and discussion

Fig.1 (a) shows the SRIM 2010 [26] simulated results of Sr (360 keV) implanted into SiC. Fig. 1 (b) shows the simulated results of Xe (167 MeV) implanted into SiC. Displacement energies of 35 and 20 eV for Si and C respectively were used in the simulation [27]. Assuming that the minimum displacement per atom (dpa) of about 0.3 dpa is enough to amorphize SiC [28], it is quite clear that implantation of Sr will result in an amorphous layer of about 200 nm from the surface and Xe ions do not amorphize SiC. From Fig.1 (a), there is also evidence of Sr ions and damage deeper than those resulting from the "normal" implantation of 360 keV Sr ions. These are probably due to knock-on effects. From these results, it is quite clear that the as-implanted Sr will be embedded in the amorphous region and that this region will be extensively exposed to large amounts of energy deposition due to electronic energy loss of the penetrating Xe ions.

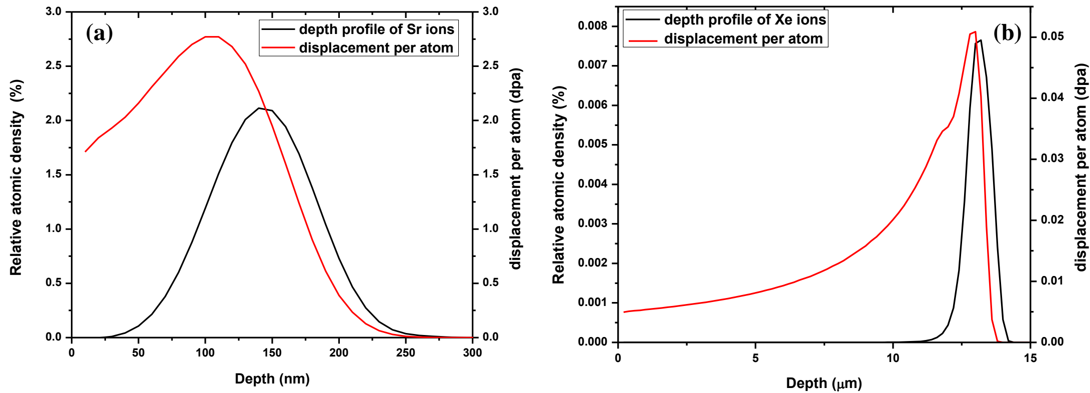

Fig. 1: *Simulated depth profiles and displacement per atom (dpa) obtained using SRIM 2010 [26], (a) 360 keV Sr depth profile and displacement per atom (b) 167 MeV Xe depth profile and displacement per atom.*

Raman spectra of the un-implanted (virgin), as-implanted and irradiated samples are shown in Fig. 2. The Raman spectrum of un-implanted SiC shows the characteristic Raman peaks of SiC [21]. Implantation of Sr into SiC at room temperature resulted in the disappearance of characteristic SiC Raman peaks between 600 to 1000 cm^{-1} and appearance of broad peak of Si-Si vibrations at around 525 cm^{-1}. This was accompanied by the damaged SiC band at around 800 cm^{-1} and C-C vibrations at around 1425 cm^{-1}. These changes indicate the amorphization of SiC layer after implantation.

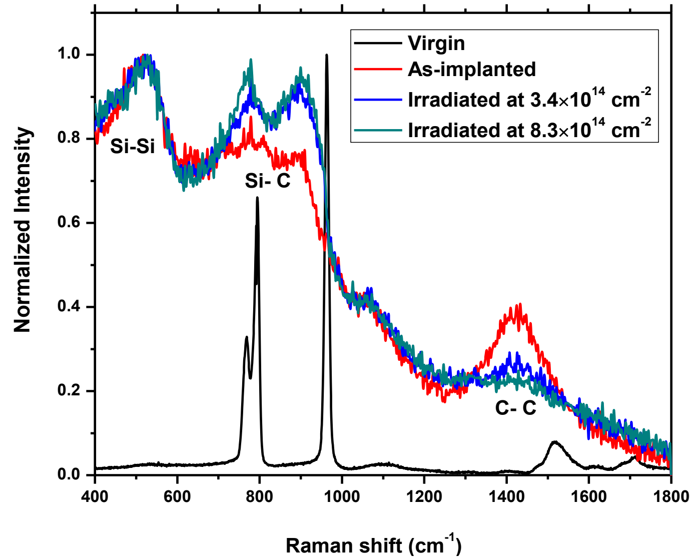

Fig. 2: *Raman spectra of the virgin SiC (virgin), implanted with 360 keV Sr ions (as-implanted), implanted with Sr then irradiated with 167 MeV Xe ions to a fluence of 3.4×10^{14} cm^{-2} and 8.3×10^{14} cm^{-2}.*

Irradiation of the implanted SiC with Xe (167 MeV) ions at room temperature to a fluence of 3.4×10^{14} cm^{-2} and 8.3×10^{14} cm^{-2} caused the partial reappearance of broad SiC Raman characteristic peaks at around 780 and 900 cm^{-1} with the Si-Si (around 525 cm^{-1}) and C-C (around 1425 cm^{-1}) peaks still present. The appearance of broader characteristic SiC peaks indicates some limited recrystallization of the initially amorphous SiC layer. Similar recrystallization of SiC implanted with different implanted ions after SHIs irradiation has been reported previously [21,22]. In these previous studies, the recrystallization was found to be due to SHIs irradiation causing the formation of randomly oriented crystallites embedded in amorphous SiC. The similarities of the reported Raman results with our current Raman results suggest that our irradiated amorphous SiC layer was also composed of randomly oriented crystallites embedded in amorphous SiC.

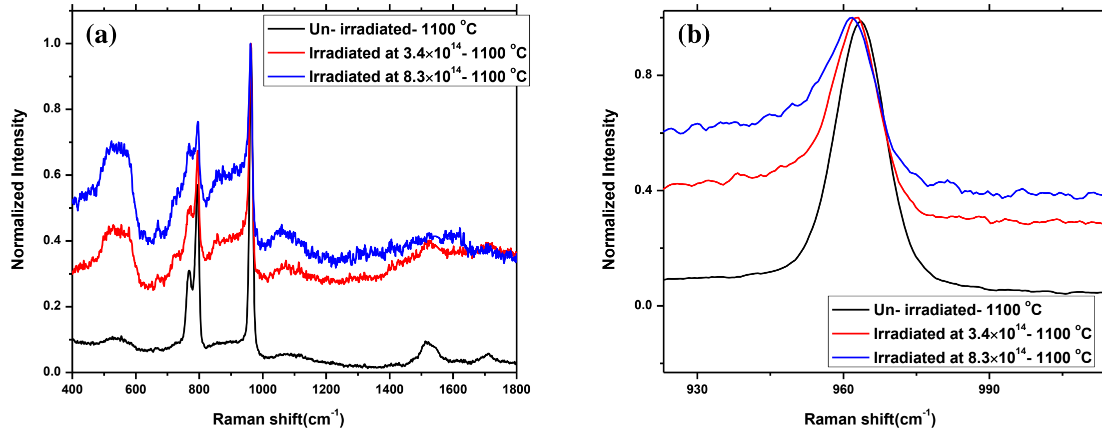

Fig. 3: ***(a)*** *Raman spectra of SiC implanted with Sr at room temperature and annealed at 1100 °C (un-irradiated - 1100 °C), implanted and then irradiated with Xe (167 MeV) ions to fluences of* 3.4×10^{14} *cm*$^{-2}$ *and* 8.3×10^{14} *cm*$^{-2}$ *and annealed at 1100 °C,* ***(b)*** *longitudinal optic (LO) phonon peaks for all samples.*

Raman spectra of irradiated and un-irradiated but implanted with Sr samples after annealing at 1100 ºC are shown in Fig. 3. Annealing the samples at 1100 ºC resulted in the reappearance of Raman characteristic peaks of SiC. The un-irradiated but implanted with Sr samples fully recrystallized resulting in the disappearance of Si-Si and C-C peaks. The irradiated samples poorly recrystallized resulting in the appearance of Raman SiC characteristic peaks with broad Si-Si peak (at about 545 cm^{-1}) and C-C peak (at 1520 cm^{-1}) still present.

It is known that SiC gives Raman scattering from a transverse optic (TO) phonon at approximately 790 cm^{-1} and a longitudinal optic phonon (LO) at 973 cm^{-1} [29]. These two peaks are slight different from Raman peaks for the un-implanted SiC (virgin) that used in this study. Raman peaks for the virgin samples showed the TO phonon mode at approximately 794 cm^{-1} and the LO phonon mode at 964 cm^{-1} (see Fig. 2). At 1100 ºC, the observed TO and LO peaks positions for un-irradiated sample were in the same positions as those of the virgin SiC. For the SHI irradiated samples, it can be observed that two distinct TO and LO peaks of SiC were both quite broad. These two peaks are forbidden in large crystals [29,30]. Thus, it can be regarded as SHI irradiated SiC were poorly crystallized with small SiC crystallites imbedded in amorphous SiC. The LO phonon at 964 cm^{-1} shifted down to 962 cm^{-1} and 961 cm^{-1} for irradiated samples at fluences of 3.4×10^{14} cm^{-2} and 8.3×10^{14} cm^{-2} respectively, which was probably due to the small crystallites which formed within the amorphous region of SiC [30]. A larger

shift toward lower wavenumber appeared in the sample irradiated to a higher fluence (8.3×10^{14} cm^{-2}) indicating smaller crystallites as shown in Fig 3(b). These variations in Raman peak shifts were accompanied by an increase in the full width at half maximum (FWHM) of the SiC Raman prominent peak (around 960 cm^{-1}) from 9.4 cm^{-1} (virgin) to 11.6 cm^{-1} for un-irradiated, 11.8 cm^{-1} and 19.6 cm^{-1} for samples irradiated to fluences of 3.4×10^{14} cm^{-2} and 8.3×10^{14} cm^{-2} respectively. The FWHM of the un-irradiated sample was narrower compared to the irradiated samples. This confirms that annealing the un-irradiated but implanted with Sr samples at 1100 °C resulted in larger crystallites compared to irradiated samples annealed in the same conditions [31]. This is rather surprising, as the irradiated samples had already partial recrystallized after irradiation while the un-irradiated sample was fully amorphous. Therefore, the recrystallization in these samples are different. This might be due to the difference in Sr impurities in the Xe-irradiated samples. The different Sr concentrations will be explained later in the RBS results. In general, impurities can usually retard the recrystallization process and inhibit crystal growth [32, 33].

The recrystallization observed by Raman spectroscopy in Fig. 3 is also evident in the SEM images shown in Fig. 4. After implantation the surfaces were featureless, as it is typical of bombardment induced amorphous SiC wafers [3]. As can be seen from Fig. 4 (a) and (b), annealing of the un-irradiated but implanted with Sr samples resulted in crystal regrowth and recrystallization competing with each other, eventually resulting in a polycrystalline surface layer with pores in it. The surface of the annealed irradiated samples (Fig. 4 (c) and (d)) shows no major changes as compared to the irradiated samples before annealing (not shown). The lack of changes on the irradiated sample surface implies that the nano-crystallites are below the SEM detection limit. These nano-crystallites clearly appeared after annealing the irradiated samples at 1200 ºC as seen in Fig. 5(b) and (c). Also more pores appeared on the surface. Comparing the results in Fig. 4(c and d) and Fig. 5(b and c) shows that the increase in temperature which increases the mobility of atoms led to the increase in average crystal size, in line with crystal growth theory [32,33]. At 1200 ºC, Raman peaks showed increased narrowing of the TO and LO mode peaks of SiC for irradiated samples indicating more recrystallization at this temperature as shown in Fig. 6.

A comparison between these SEM images with the Raman results clearly shows a difference in the recrystallization between un-irradiated and irradiated samples. Apart from the influence of impurities as mentioned above, this difference in the recrystallization might also be due to the fact that the initial surfaces/layers were in different states before annealing, i.e. the un-irradiated but implanted with Sr samples were amorphous while the irradiated samples were partially recrystallized.

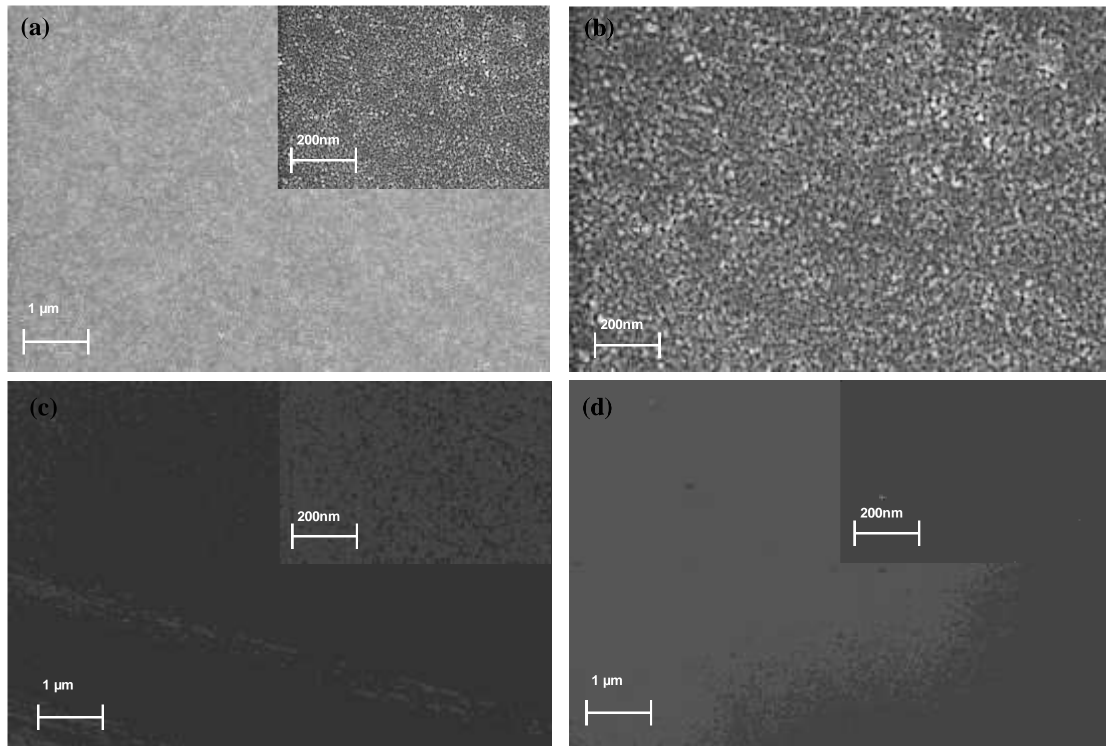

Fig. 4: *SEM micrographs of samples annealed at 1100 ºC. (a) Un-irradiated but implanted with Sr, (b) A high magnification image of the same sample which shows that pores were present. (c) and (d) Irradiated with Xe to a fluence of* 3.4×10^{14} cm^{-2} *and* 8.3×10^{14} cm^{-2} *respectively.*

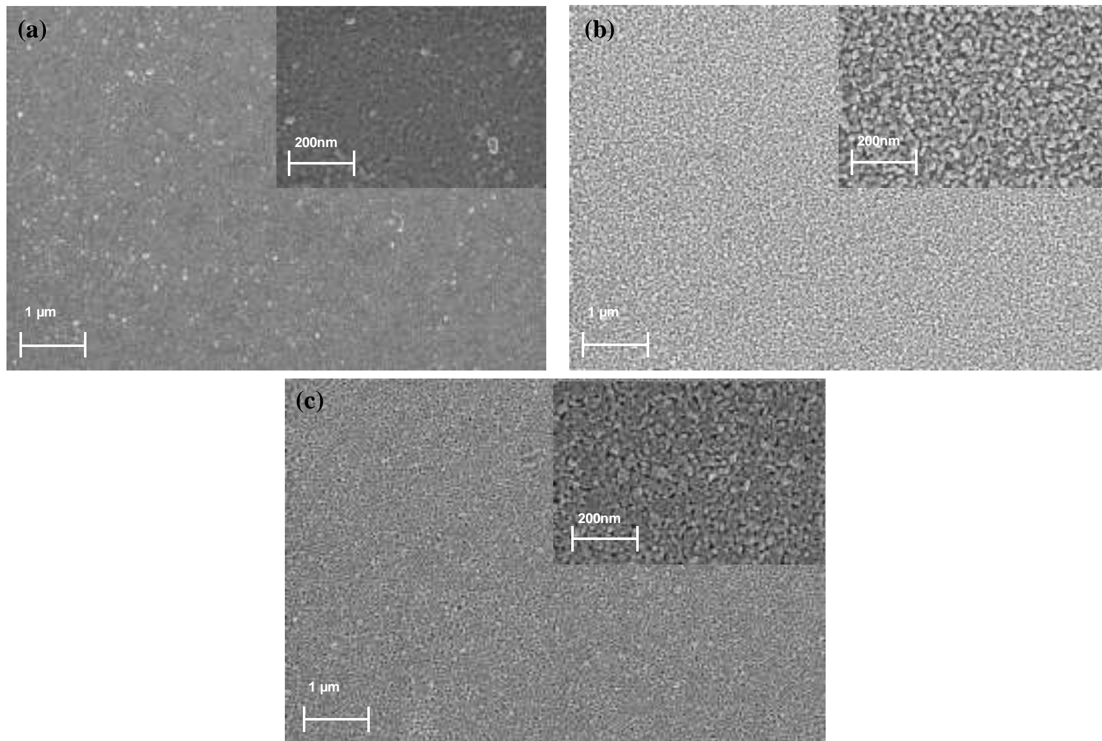

Fig. 5: *SEM micrographs of samples annealed at 1200 °C. (a) Un-irradiated but implanted with Sr. (b) and (c) Irradiated samples with Xe to a fluence of* 3.4×10^{14} *cm*$^{-2}$ *and* 8.3×10^{14} *cm*$^{-2}$ *respectively.*

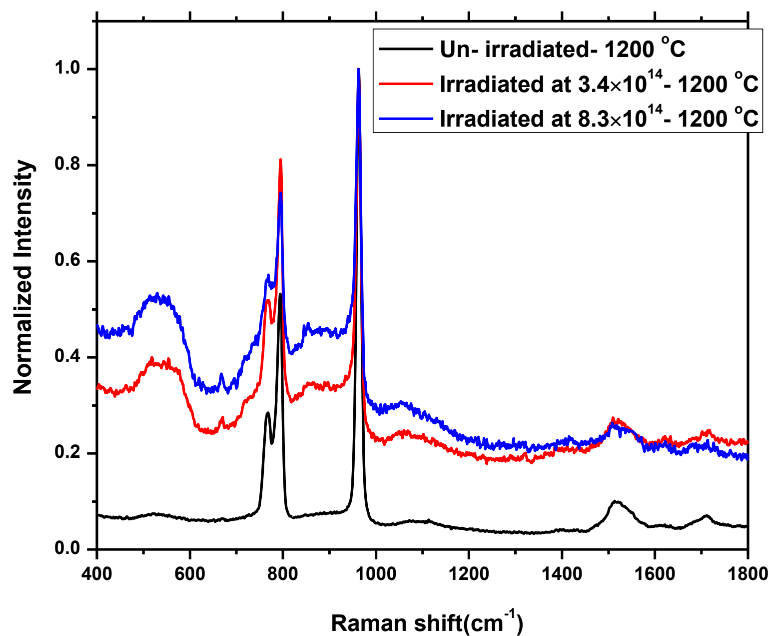

Fig. 6: *Raman spectra of SiC implanted with Sr at room temperature then annealed at 1200 °C (un-irradiated - 1200 °C), implanted and then irradiated with Xe ions to fluences of* 3.4×10^{14} *cm*$^{-2}$ *and* 8.3×10^{14} *cm*$^{-2}$ *and annealed at 1200 °C.*

The SEM micrographs of both irradiated and un-irradiated samples after sequentially annealing up to 1300 °C and 1400 °C are shown in Fig. 7 and Fig. 8 respectively. The micrographs show that the SiC crystallites increased in size with the increase in annealing temperature. As discussed above, this is due to crystal growth [32,33]. More pores/openings appeared in the SHI irradiated samples as seen in Fig. 7(b) and (c). In Fig. 8 (i.e. annealed at 1400 °C) the average crystallite size became slightly larger with fewer and smaller pores compared to the equivalent samples at lower temperatures. In contrast, these pores were larger and clearly visible in the un-irradiated but implanted with Sr samples annealed at 1100 °C (Fig. 4(a) (b)) and in irradiated samples annealed at 1300 °C (Fig. 7 (b) and (c)). The same explanation of crystal growth used above is also applicable here.

Raman spectra of the un-irradiated and irradiated samples after sequentially annealing up to 1300 °C and 1400 °C are shown in Fig. 9 (a) and (b) respectively. The Raman peaks show more narrowing of TO and LO peaks for all the samples. This narrowing of FWHM indicates an increase in grain size during recrystallization of the samples [31].

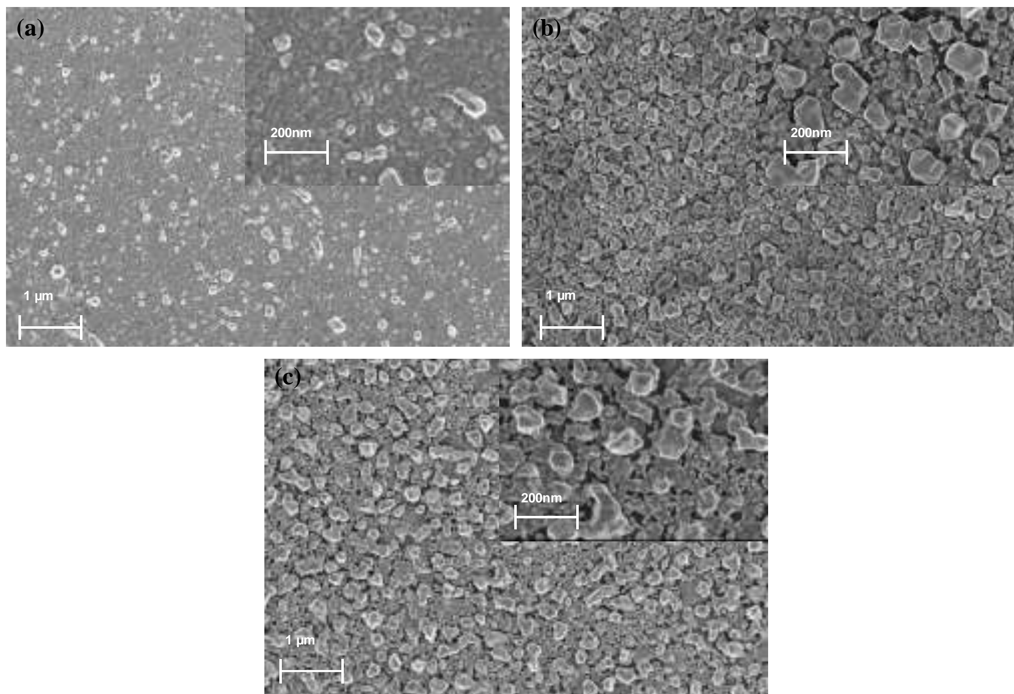

Fig. 7: *SEM micrographs of samples annealed at 1300 °C. (a) Un-irradiated but implanted with Sr. (b) and (c) Irradiated samples with Xe to a fluence of* 3.4×10^{14} cm^{-2} *and* 8.3×10^{14} cm^{-2} *respectively.*

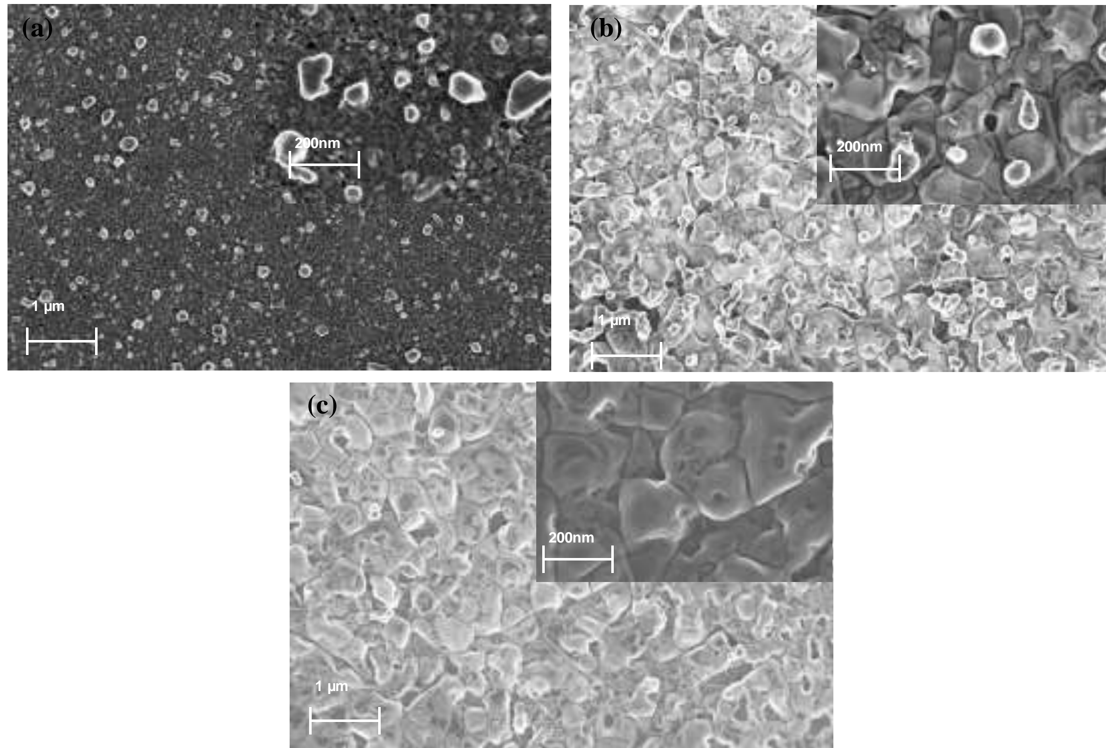

Fig. 8: *SEM micrographs of samples annealed at 1400 °C. (a) Un-irradiated but implanted with Sr. (b) and (c) Irradiated samples with Xe to a fluence of 3.4×10^{14} cm^{-2} and 8.3×10^{14} cm^{-2} respectively.*

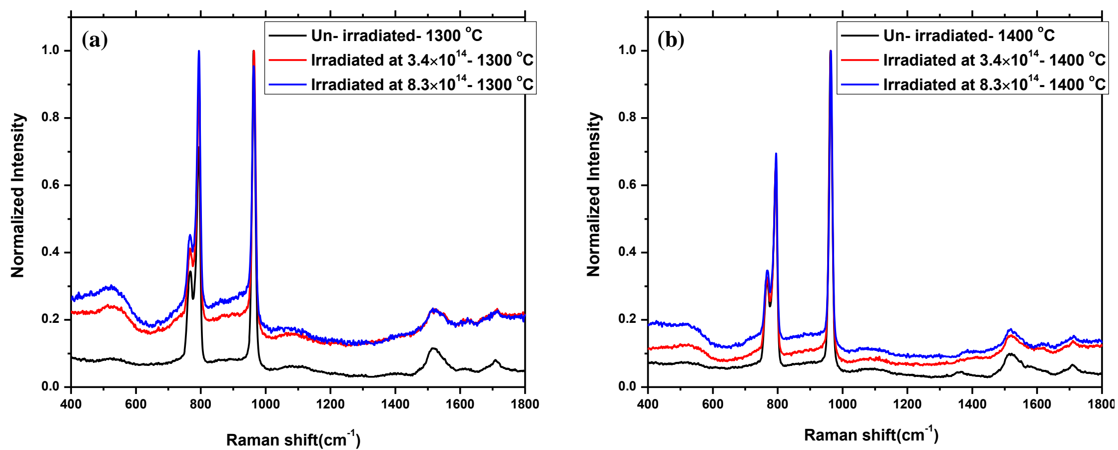

Fig. 9: *Raman spectra of un-irradiated but implanted with Sr and irradiated SiC samples annealed at (a) 1300 and (b) 1400 °C.*

Raman spectra of the un-irradiated but implanted with Sr and irradiated samples after sequentially annealing up to 1500 ºC are shown in Fig. 10. Annealing the un-irradiated but implanted with Sr and irradiated samples at 1500 ºC resulted in the appearance of

peaks around 1360 cm^{-1} and 1580 cm^{-1} corresponding to D and G peaks respectively. The appearance of these peaks indicates the presence of a carbon layer on the sample surfaces. These peaks were not observed after annealing at temperatures from 1100 to 1400 ºC (as seen in Fig. 3, 6 and 9).

The SEM micrographs of both irradiated and un-irradiated samples after sequentially annealing up to 1500 ºC are shown in Fig. 11. Some of the crystallites can be seen to be protruding from the SiC substrate surface. This effect was more visible on the un-irradiated but implanted with Sr samples with their larger crystallite sizes. This can be explained in terms of Wulff's law (i.e. the preferential growth of a crystal surface with a lower surface energy compared to another surface with a higher surface energy) [34,35]. In addition, thermal etching can play a contributing role at this temperature for both samples [35]. Fig 11(a) shows thin strands of graphitic material between the SiC crystallites and clusters with few and very small pores on the surface after annealing at 1500 °C.

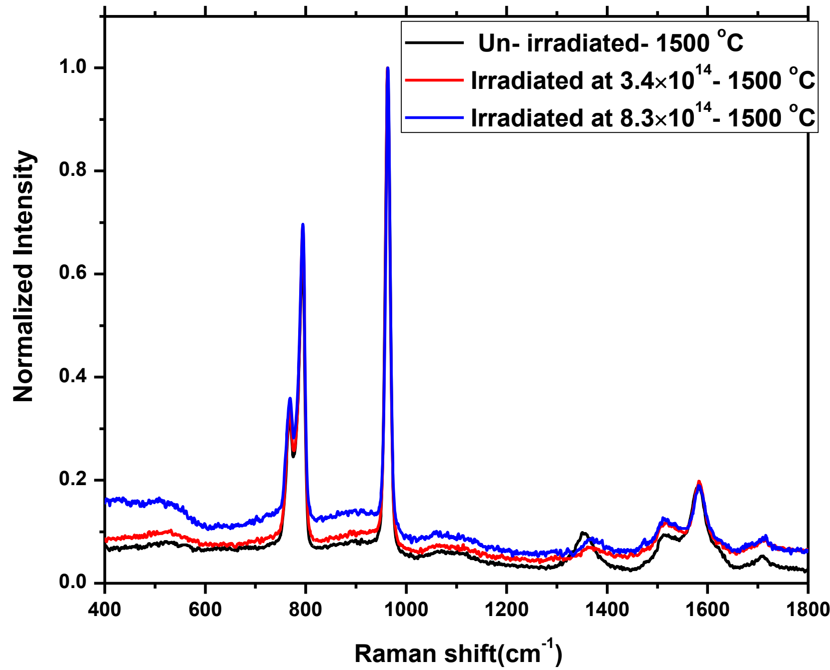

Fig. 10: *Raman spectra of SiC implanted with Sr at room temperature and then sequentially annealed up to 1500 °C (Un-irradiated - 1500 ºC), implanted and then irradiated to fluences of 3.4×10*^{14} *cm*$^{-2}$ *and 8.3×10*^{14} *cm*$^{-2}$ *and sequentially annealed up to 1500 ºC.*

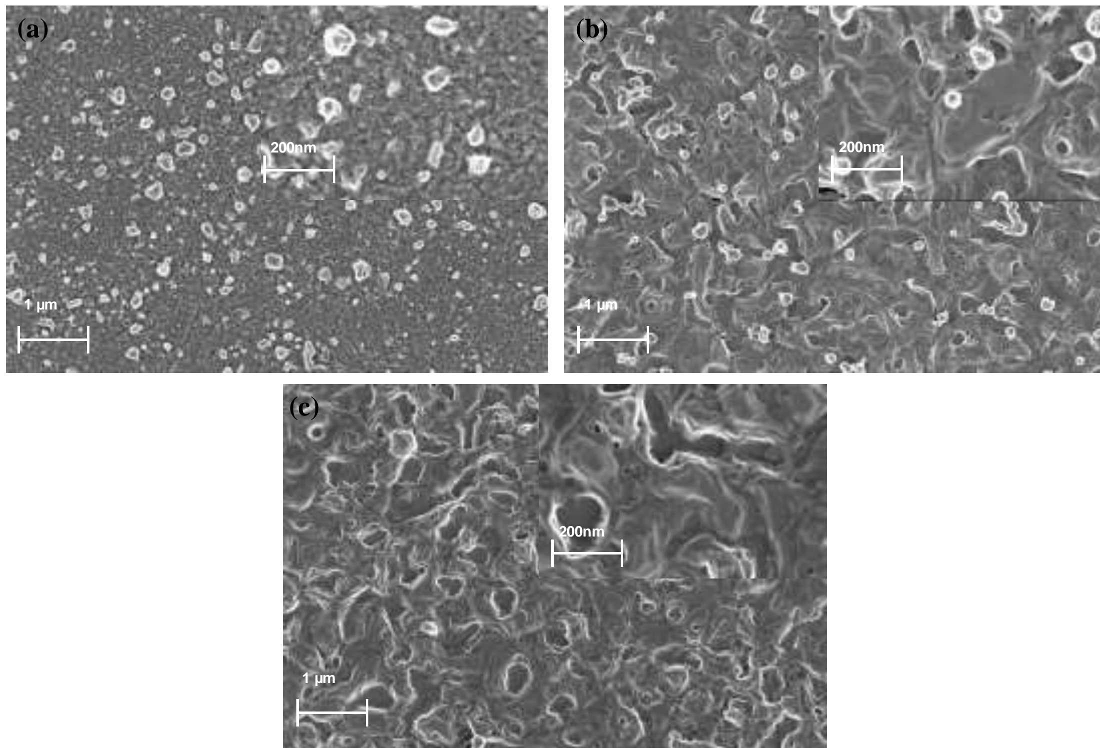

***Fig. 11**: SEM micrographs of irradiated and un-irradiated samples but implanted with Sr after sequentially annealing up to 1500 ^{o}C (a) Un-irradiated but implanted with Sr. (b) and (c) Irradiated with Xe ions to a fluence of 3.4×10^{14} cm^{-2} and 8.3×10^{14} cm^{-2} respectively.*

Fig. 12 shows the RBS spectra of SiC (both un-irradiated and irradiated samples) after sequentially annealing from 1100 to 1500 ^{o}C for 5 hours in steps of 100 ^{o}C. The Sr are not included in Fig. 12. Arrows in Fig. 12 indicate the Si and C surface channel positions. Sequential annealing the samples up to 1500 ^{o}C resulted in the accumulation of carbon on the SiC sample surfaces. This was accompanied by the shift of the Si surface energy channel position to lower energy channels indicating the presence of a carbon layer on the SiC surface. The free carbon on the surface was due to thermal decomposition of SiC and sublimation of silicon thus leaving a free carbon layer on the SiC surfaces. The decomposition of implanted SiC layers has been reported to occur at temperatures above 1400 °C [12,35,36]. The decomposition of SiC observed in RBS at 1500 ^{o}C correlates with Raman results (Fig. 10) which showed the appearance of the D and G peaks at this temperature and with the SEM image shown in Fig. 11(a).

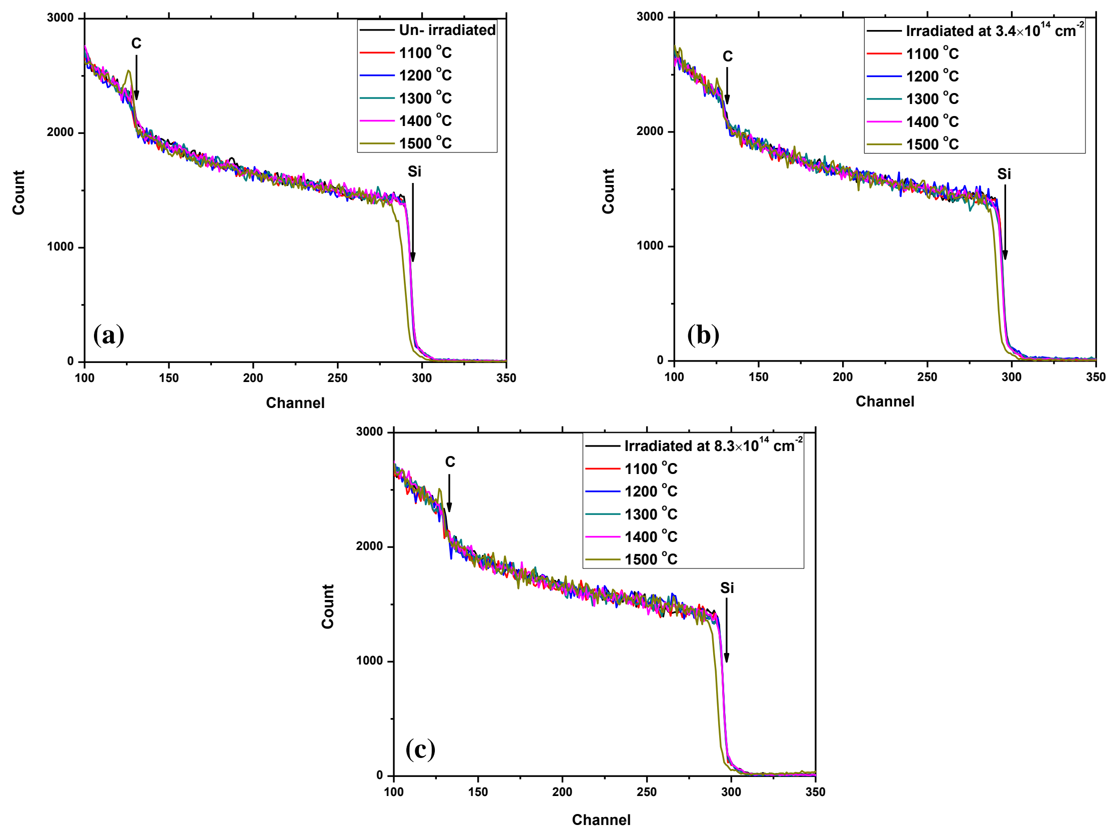

Fig. 12: *RBS spectra of irradiated and un-irradiated SiC samples but implanted with Sr before and after sequentially annealing up to 1500 °C. (a) Un-irradiated but implanted with Sr. (b) and (c) Implanted with Sr then irradiation with Xe at room temperature to a fluence of* 3.4×10^{14} *cm*$^{-2}$ *and* 8.3×10^{14} *cm*$^{-2}$ *respectively.*

Migration behaviour of Sr implanted into SiC was investigated after irradiation and sequential annealing. No migration of implanted Sr was observed in the un-annealed SHIs irradiated sample. Similar results have been reported for other implanted fission products surrogates are SHIs irradiations [21,22,24].

The strontium depth profiles of irradiated and un-irradiated samples after sequentially annealing at temperatures ranging from 1100 to 1500 ºC for 5 hours are shown in Fig. 13. Annealing the un-irradiated samples at 1100 ºC resulted in strong migration of Sr towards the surface accompanied by significant loss (of about 25%) of implanted Sr. This was due to the presence of pores in the surface extending into the implanted layer – see Fig. 4(b). At temperatures of 1200 °C and above, further loss of Sr through the surface was observed in the un-irradiated sample - see Fig. 13 (a) and Fig. 14. As mentioned above, the growth of the crystallites led to the closure of the pores through

which the sublimated Sr can escape into the vacuum. The un-irradiated samples retained about 25% of Sr ions after sequentially annealing up to 1500 ºC. This was due to very small pores as seen in Fig. 11 (a), compared to the un-irradiated sample annealed at 1100 ºC in Fig. 4(a) and (b). This reduction in pore size is due to the grain growth of the SiC crystals. In the irradiated samples, Sr migrate towards the surface and into the undamaged bulk after annealing at 1100 ºC as shown in Fig. 13(b) and (c). This migration was accompanied by slightly loss of about 3% and no loss of implanted Sr for the samples irradiated at 3.4×10^{14} cm^{-2} and 8.3×10^{14} cm^{-2} respectively. The different amounts of retained strontium after annealing were due to the difference in surface structure of the samples. Annealing the irradiated samples at 1200 ºC shows significant loss of about 30% and 70% of Sr for the samples irradiated at 3.4×10^{14} cm^{-2} and 8.3×10^{14} cm^{-2} respectively. This was due to the presence of pores on the surface of irradiated samples as seen in Fig. 5 (b) and (c). No Sr were retained in the 8.3×10^{14} cm^{-2} and 3.4×10^{14} cm^{-2} irradiated samples after annealing at 1300 and 1400 ºC respectively - see Fig. 14. A previous study by Friedland et *al.* [37,38] found that the implanted strontium is trapped and released by defect complexes at different temperatures, thereby not exhibiting normal Fickian diffusion which can be analyzed by the conventional equations and methods.

The small loss of Sr in the un-irradiated samples and the high loss of Sr in the irradiated samples after sequentially annealing up to 1400 ºC was due to the different structures in the annealed un-irradiated and irradiated samples. As discussed above in Fig. 3, annealing the un-irradiated samples at 1100 ºC led to the formation of rather large grains while annealing the irradiated samples produced fine grained structures. Annealing the un-irradiated samples at 1200 and 1300 ºC led to the formation of small sized pores on the surface while annealing the irradiated samples produced large sized pores as shown in Fig 5 and 7. This resulted in high amount of Sr released in the latter samples. From these results, it is quite clear that Sr loss is favored in the irradiated SiC structure.

The low concentration of impurities in irradiated samples after annealing at 1200, 1300 and 1400 ºC resulted in faster grain growth as shown in Fig. 5(b and c), 7(b and c) and 8 (b and c) respectively. As discussed above, impurities usually inhibit crystal growth [32,33].

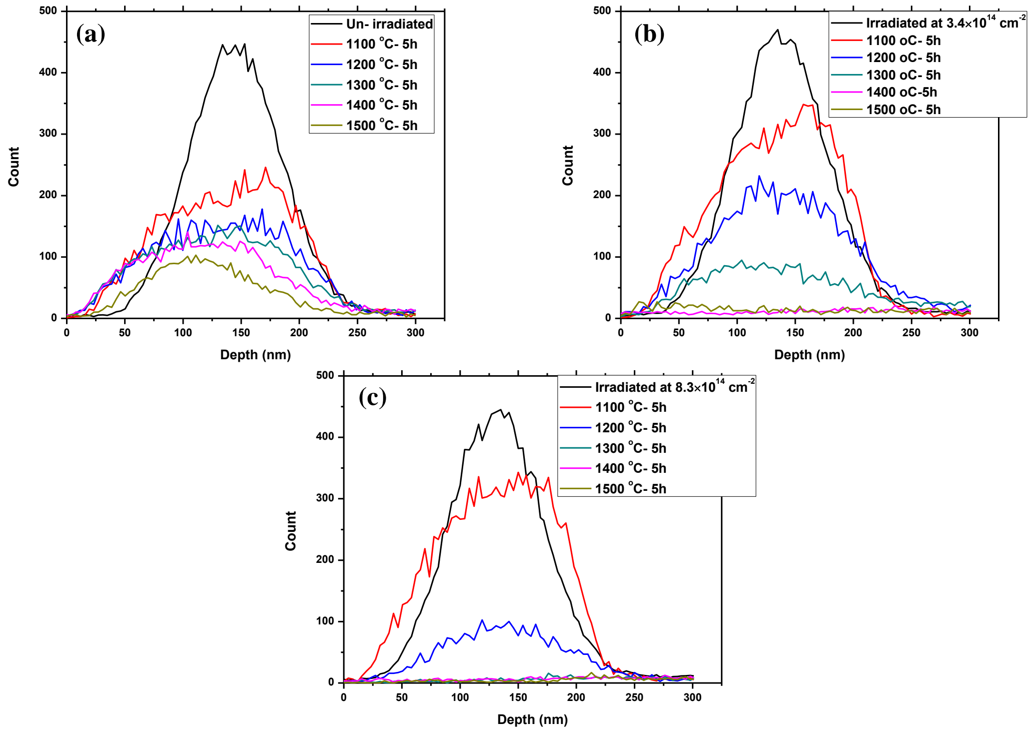

Fig. 13: *RBS Sr depth profiles for irradiated and un-irradiated samples before and after annealing. (a) Sr depth profiles for un-irradiated samples. (b) and (c) Sr depth profiles for irradiated samples with Xe at room temperature to a fluence of 3.4×10^{14} cm^{-2} and 8.3×10^{14} cm^{-2} respectively.*

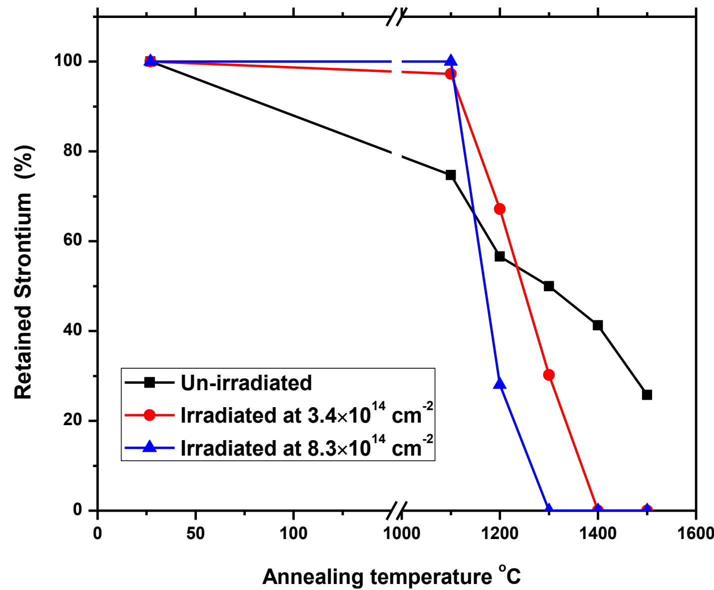

Fig. 14: *The retained ratio of strontium in irradiated and un-irradiated samples before and after sequential annealing up to 1500 ^{0}C.*

4. Conclusion

The microstructure of the substrate and the migration behavior of strontium (Sr) implanted into polycrystalline CVD SiC was investigated using RBS, Raman and SEM. Sr^{+} ions of 360 keV were implanted into polycrystalline SiC to a fluence of 2×10^{16} cm^{-2} at room temperature. Some of the implanted samples were irradiated with xenon (Xe) ions of 167 MeV to a fluence of 3.4×10^{14} cm^{-2} and 8.3×10^{14} cm^{-2} at room temperature. Both the as-implanted, implanted then irradiated samples were isochronally annealed at temperatures ranging from 1100 to 1500 °C in steps of 100 °C for 5 hours. Implantation of Sr at room temperature amorphized the near surface implanted region of the SiC substrate, while SHIs irradiation of the as-implanted samples caused some limited recrystallization of the amorphized layer. Recrystallization was already taking place after annealing at 1100 °C in the irradiated and un-irradiated samples. At this temperature, the un-irradiated but implanted samples recrystallized more than the irradiated samples. Migration of implanted Sr was already taking place at 1100 °C in both irradiated and un-irradiated but implanted with Sr samples. The un-irradiated samples showed a loss of 25% of Sr after annealing at 1100 °C. The irradiated samples showed a slight Sr loss of about 3% and no loss for samples irradiated at 3.4×10^{14} cm^{-2} and 8.3×10^{14} cm^{-2} respectively. The un-irradiated but implanted with Sr sample retained about 25% of Sr ions after having been sequentially annealed up to 1500 °C, while no Sr ions were retained in the 8.3×10^{14} cm^{-2} and 3.4×10^{14} cm^{-2} irradiated samples after annealing at 1300 and 1400 °C respectively. These differences in the migration behavior of Sr is due to the difference in SiC structure and recrystallization in the irradiated and un-irradiated but implanted with Sr samples. Decomposition of SiC were observed after annealing at 1500 °C for all samples. The results show that more Sr was released in the irradiated SiC samples.

5. References

[1] D.A. Petti, P.A. Demkowicz, J.T. Maki, R.R. Hobbins, TRISO-Coated particle fuel performance, Compr. Nucl. Mater. 3 (2012) 151–213.

[2] K. Verfondern, H. Nabielek, J.M. Kendall, Coated particle fuel for high Temperature gas cooled reactors, Nucl.Eng. Des. 39(2007) 603–616.

[3] J.B. Malherbe, Topical Review: Diffusion of fission products and radiation damage in SiC, J. Phys. D Appl. Phys. 46 (2013) 473001 (27 page).

[4] J.B. Malherbe, E. Friedland, N.G. van der Berg, Ion beam analysis of materials in the PBMR reactor, Nucl. Instrum. Methods Phys. Res. B 266 (2008) 1373-1377.

[5] N. G. van der Berg, J. B. Malherbe, A. J. Botha and E. Friedland, SEM analysis of the microstructure of the layers in triple-coated isotropic (TRISO) particles, Surf. Interface Anal. 42 (2010) 1156–1159.

[6] L.L. Snead, T. Nozawa, Y. Katoh, T.-S. Byun, S. Kondo, D.A. Petti, Handbook of SiC properties for fuel performance modeling, J. Nucl. Mater. 371 (2007) 329-377.

[7] H. Abderrazak, E. S. Bel Hadj, R. Gerhardt (Ed.), Silicon carbide: synthesis and properties, properties and applications of silicon carbide, InTech, (2011). DOI: 10.5772/15736. Available from: https://mts.intechopen.com/books/properties-and-applications-of-silicon-carbide/silicon-carbide-synthesis-and-properties.

[8] E. Lopez-Honorato, C. Brigden, R.A. Shatwell, H. Zhang, I. Farnan, P. Xiao, P. Guillermier, J. Somers, Silicon carbide polytype characterisation in coated fuel particles by Raman spectroscopy and ^{29}Si magic angle spinning NMR, J. Nucl. Mater. 433 (2013)199-205.

[9] P. Krautwasser, G.M. Begun, P. Angelini, Raman spectral characterization of silicon carbide nuclear fuel coatings, J. Am. Ceram. 66 (1983) 424-434.

[10] TECDOC- 978, Fuel performance and fission product behaviour in gas-cooled reactors, Tech. rep, IAEA, Vienna, 1997. Available from: http://www-pub.iaea.org/books/IAEABooks/5633/Fuel-Performance-and-Fission-ProductBehaviour-in-Gas-Cooled-Reactors.

[11] H. Nabielek, P.E. Brown, P. Offermann, Silver release from coated particle fuel, Nucl. Technol. 35 (1977)483-493.

[12] E. Friedland, J.B. Malherbe, N.G. van der Berg, T. Hlatshwayo, A.J. Botha, E. Wendler, W. Wesch, Study of silver diffusion in silicon carbide, J. Nucl. Mater. 389 (2009) 326–331.

[13] H.J. MacLean, Silver Transport in CVD Silicon Carbide, PhD Thesis, MIT, Department of Nuclear Engineering, 2004.

[14] E. Lo´pez-Honorato, H. Zhang, D. Yang, P. Xiao, Silver diffusion in silicon carbide coatings, J. Am. Ceram. Soc. 94 (2011) 3064–3071.

[15] S. Dwaraknath, G. Was, Development of a multi-layer diffusion couple to study fission product transport in b-SiC, J. Nucl. Mater. 444 (13) (2014) 170- 174.

[16] Anon, (2016). [online]Availableat: https://www.hydrogen.energy.gov/pdfs/national_h2_roadmap.pdf [Accessed 10 Jun. 2016].

[17] S. Dwaraknath, G. Was, The diffusion of cesium, strontium, and europium in silicon carbide, J. Nucl. Mater. 476 (2016) 155-167.

[18] D. Petti, J. Buongiorno, J. Maki, R. Hobbins, G. Miller, Key differences in the fabrication, irradiation and high temperature accident testing of US and German TRISO-coated particle fuel, and their implications on fuel performance, Nucl. Eng. Des. 222 (2-3) (2003) 281-297.

[19] S.J. Zinkle, V.A. Skuratov, D.T. Hoelzer, On the conflicting roles of ionizing radiation in ceramics, Nucl. Instrum. Methods Phys. Res., B191 (2002) 758- 766.

[20] E.V. Kalinina, V.A. Skuratov, A.A. Sitnikova, E.V. Kolesnikova, A.S. Tregubova, M.P. Scheglov, Structural peculiarities of 4H-SiC irradiated by Bi ions, Semiconductors 41 (2007) 376–380.

[21] T. T. Hlatshwayo, J. H. O'Connell, V. A. Skuratov, E. Wendler, E. G. Njoroge, M. Mlambo, J. B. Malherbe, Comparative study of the effect of swift heavy ion irradiation at 500 ºC and annealing at 500 ºC on implanted silicon carbide. RSC Adv, 6 (2016) 68593-68598.

[22] T. T. Hlatshwayo, J. H. O’Connell, V.A. Skuratov, M. Msimanga, R. J. Kuhudzai, E.G. Njoroge, J.B. Malherbe, Effect of Xe ion (167 MeV) irradiation on polycrystalline SiC implanted with Kr and Xe at room temperature, J. Phys. D: Appl. 48 (2015) 465306.

[23] A. Debelle, M. Backman, L. Thome, W. J. Weber, M. Toulemonde, S. Mylonas, A. Boulle, O. H. Pakarinen, N. Juslin, F. Djurabekova, K. Nordlund, F. Garrido, and D. Chaussende, Combined experimental and computational study of the

recrystallization process induced by electronic interactions of swift heavy ions with silicon carbide crystals. Physics Review B 86 (2012)100102.

[24] A. Audren, A. Benyagoub, L. Thome and F. Garrido, Ion implantation of iodine into silicon carbide: influence of temperature on the produced damage and on the diffusion behavior, Nucl. Instrum. Methods Phys. Res. B. 266 (2008) 2810–2813.

[25] B. Leng, H. Ko, T.J. Gerczak, J. Deng, A.J. Giordani, J.L. Hunter Jr, D. Morgan, I. Szlufarska, K. Sridharan, Effect of carbon ion irradiation on Ag diffusion in SiC, J. Nucl. Mater. 471(2016)220-232.

[26] J.F. Ziegler, M.D. Ziegler, J.P. Biersack, SRIM – The stopping and range of ions in matter (2010), Nucl. Instrum. Methods Phys. Res. Sect. B Beam Interact. Mater. Atoms 268 (11–12) (2010) 1818–1823.

[27] W.J. Weber, F. Gao, R. Devanathan, W. Jiang, The efficiency of damage production in silicon carbide**,** Nucl. Instrum. Methods Phys. Res. B218 (2004) 68.

[28] W.J. Weber, N. Yu, L.M. Wang, Structure and properties of ion-beam-modified (6H) silicon carbide**,** J. Nucl. Mater. 53 (1998) 253.

[29] D.W. Feldman, James H. Parker, Jr., W.J. Choyke and L. Patrick, Phonon dispersion curves by Raman scattering in SiC, polytypes 3C, 4H, 6H, 15R and 21R. Phys. Rev., 173 (1968) 787.

[30] H.Richter, Z.P.Wang and L.Ley, The one phonon Raman spectrum in microcrystalline silicon. Solid State Commun., 39 (1981) 625.

[31] X. Qiang, H. Li, Y. Zhang, S. Tian, J. Wei, Synthesis and Raman scattering of SiC nanowires decorated with SiC polycrystalline nanoparticles. Materials Letters 107 (2013) 315–317.

[32] W. K Burton, N Cabrera and F C. Frank, The growth of crystals and the equilibrium structure of their surfaces. Phil. Trans. Roy. Soc. 243A (1951) 299- 358.

[33] J.P. Hirth and G.M. Pound, Coefficients of evaporation and condensation. J. Phys. Chem. 64 (1960) 619–626.

[34] G. Wulff, Xxv. Zur Frage der Geschwindigkeit des Wachsthums und der Auflösung der Krystallflächen, Z. Krist. 34 (1) (1901) 449-530.

[35] N.G. van der Berg, J.B. Malherbe, A.J. Botha and E. Friedland. Thermal etching of SiC, Appl. Surf. Sci, 258 (2012) 5561 -5566.

[36] T.T. Hlatshwayo, J.B. Malherbe , N.G. van der Berg, A.J. Botha, P. Chakraborty, Effect of thermal annealing and neutron irradiation in 6H-SiC implanted with silver at 350° C and 600° C, Nucl. Instrum. Methods Phys. Res. B 273 (2012) 61–64.

[37] E. Friedland, N.G. van der Berg, J.B. Malherbe, E. Wendler and W. Wesch, Influence of radiation damage on strontium and iodine diffusion in silicon carbide. J. Nucl. Mater. 425 (2012) 205-210.

[38] E. Friedland, T. Hlatshwayo and N van der Berg, Influence of radiation damage on diffusion of fission products in silicon carbide. Phys. Stat. Solidi C 10 (2013) 208-215.